Figure S1_Naylor et al.

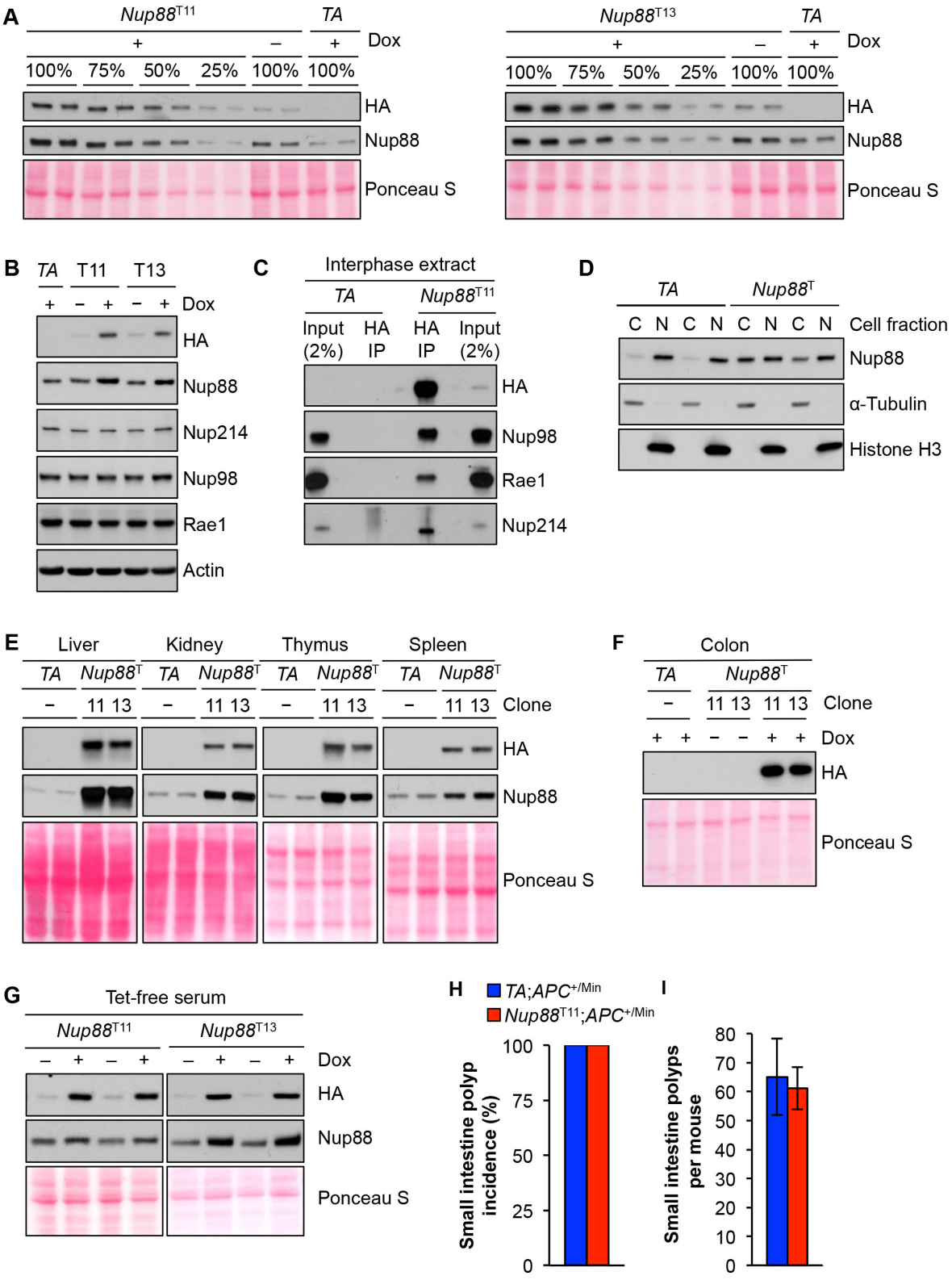

Figure S1. *Nup88* transgene expression analysis. (A) Semi-quantitative western blots for Nup88 overexpression (fold-change) in MEFs derived from *Nup88* transgenic lines 11 or 13 grown in the presence or absence of dox for 48 h. (B) Western blot analysis of various NPC components in *Nup88* transgenic MEFs. (C) Western blot analysis of G2 phase MEFs subjected to immunoprecipitation with anti-HA Affinity Matrix and analyzed for co-precipitation. (D) Western blot analysis of MEFs subjected to subcellular fractionation. C, cytoplasmic; N, nuclear. (E) Western blot analysis of tissue lysates from 6-week old dox-treated *HA-Nup88* and control (*TA*) transgenic mice. (F) Same as (E) except two *Nup88* transgenic mice did not receive dox. (G) Western blot analysis of *Nup88* transgenic MEFs grown in the presence or absence of dox using media containing tet-free serum. (H) Incidence and (I) multiplicity of colon tumors in *TA*; $APC^{+/Min}$ and $Nup88^{T11}$; $APC^{+/Min}$ mice. Data represents mean ± s.e.m. Western blots are representative of three independent experiments. Panels in (B) were taken from multiple independent gels loaded identically. $Nup88^{T}$ indicates combined transgenic lines 11 and 13.

Figure S2_Naylor et al.

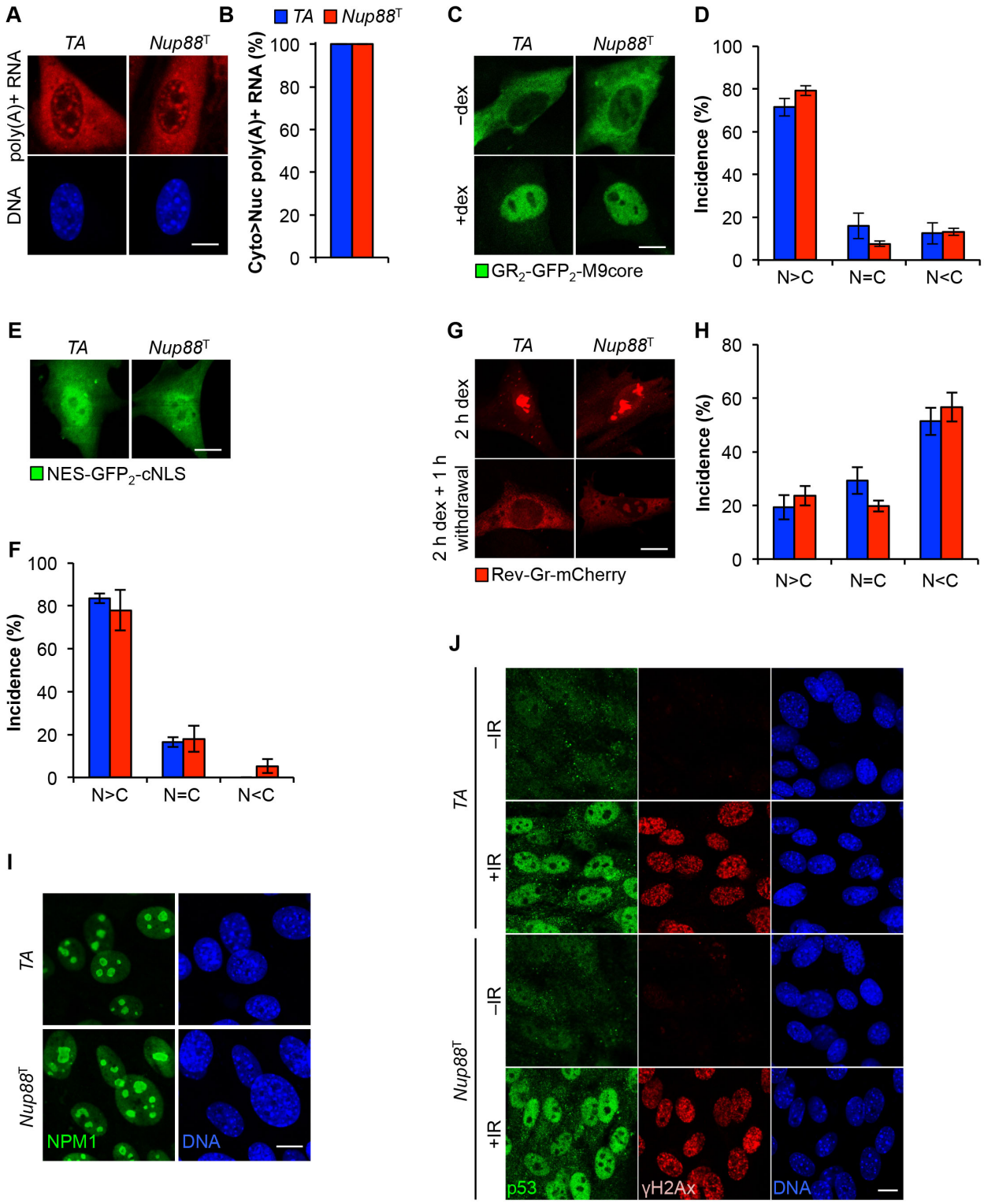

Figure S2. *Nup88* transgenic MEFs have no overt nuclear transport defects. (A) Representative

images of *TA* and *Nup88* transgenic MEFs stained for poly(A)+ RNA by *in situ* hybridization using a biotin-labeled oligo$(dT)_{50}$ probe and visualized by rhodamine-conjugated streptavidin. (B) Quantification of cells in (A) with stronger cytoplasmic poly(A)+ RNA staining in the cytoplasm versus the nucleus. (C) Representative images of MEFs expressing the Gr_2-GFP_2-M9core expression construct before or after 20 min dexamethasone (dex) treatment. (D) Quantification of M9-mediated protein import for cells in (C). (E) Representative images of MEFs expressing the NES-GFP_2-cNLS shuttle vector. (F) Quantification of NLS-mediated protein import for cells in (E). (G) Representative images of MEFs expressing the HIV-1-Rev-Gr-mCherry expression vector after 2 h dex or 2 h dex plus 1 h withdrawal. (H) Quantification of NES-mediated protein export for cells in (G). (I) Representative images of MEFs immunostained for NPM1 of the indicated genotype. (J) Representative images of MEFs immunostained for p53 and γH2Ax before or 2 h after 30 Gy irradiation of the indicated genotype. DNA in A, I, and J was visualized using Hoechst. For each experiment, three independent MEF lines were used per genotype (>25 cells per line). Data represents mean ± s.e.m. Scale bars = 10 μm. *Nup88*^{T} indicates combined transgenic lines 11 and 13.

Figure S3_Naylor et al.

A.

Mitotic MEF genotype (n)	Clone	Dox	Mitotic figures inspected	Percent aneuploid figures	s.d.	Karyotypes with indicated chromosome number							Percent mitotic figures with PMSCS	s.d.
						37	38	39	40	41	42	43		
TA+ (3)	N/A	+	150	12	2		2	6	132	7	3		5	2
Nup88 (3)	11	–	150	17	1	3	1	7	124	10	5		7	2
Nup88 (3)	11	+	150	33	3	2	6	10	100	26	4	2	13	6
Nup88 (3)	13	–	150	15	1	3	6	7	127	6	1		4	1
Nup88 (3)	13	+	150	25	1	4	5	8	113	13	6	1	6	1

B.

Mouse genotype	Clone	Mouse age (n)	Mitotic figures inspected	Percent aneuploid figures	s.d.	Karyotypes with indicated chromosome number							Percent mitotic figures with PMSCS	s.d.
						37	38	39	40	41	42	43		
TA	N/A	5 mo (6)	300	4	2		1	7	280	3			3	3
Nup88	11	5 mo (3)	150	16	3	2	9	12	111	1			8	4
Nup88	13	5 mo (3)	150	15	4	1	1	16	118	3	2		9	4

Figure S3. Nup88 overexpression causes aneuploidy. (A) Karyotype analysis of numerical chromosomal abnormalities in MEFs of the indicated genotype. (B) Same as (A) except from splenocytes harvested from 5-month old transgenic mice.

Figure S4_Naylor et al.

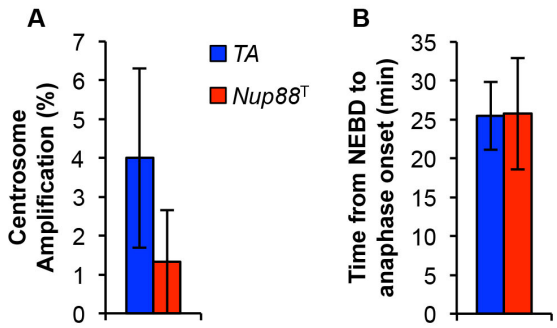

Figure S4. Nup88 overexpression does not cause centrosome amplification or alter mitotic progression. (A) Quantification of *TA* and *Nup88* transgenic MEFs with >2 γ-tubulin-positive centrosomes in metaphase. Three independent MEF lines were used per genotype (25 cells per line). (B) Analysis of duration from nuclear envelope breakdown (NEBD) to anaphase onset. 30 total cells from three independent lines were analyzed for each genotype. Error bars represent SD. *Nup88*^{T} indicates combined transgenic lines 11 and 13.

Figure S5_Naylor et al.

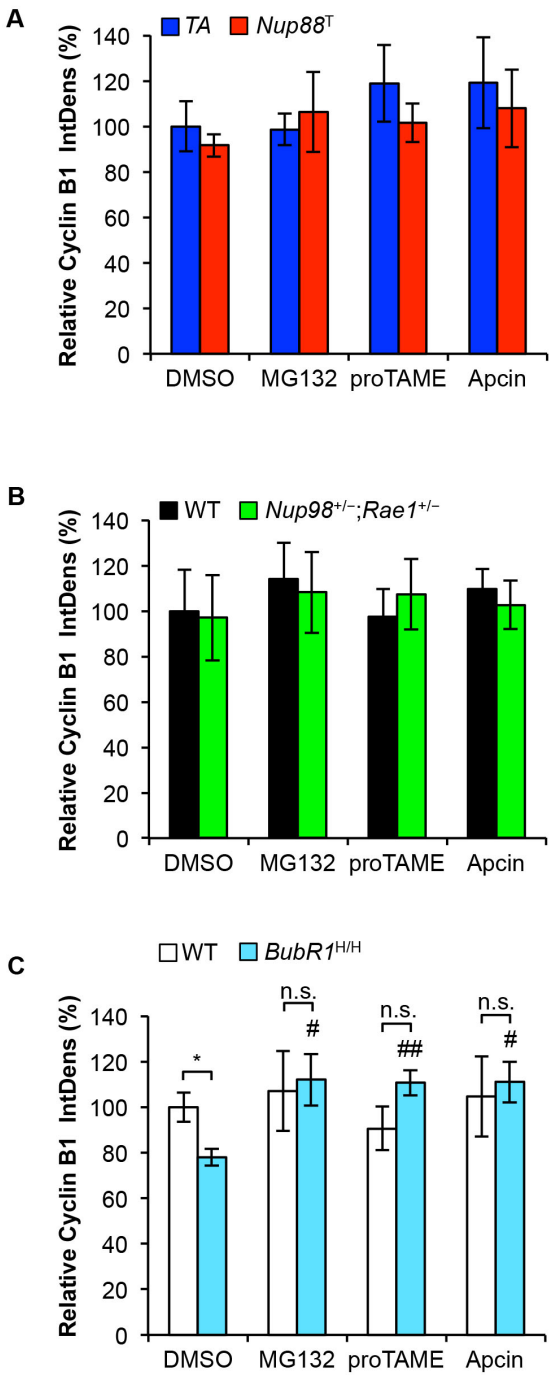

Figure S5. Apcin treatment alone is sufficient to restore Cyclin B1 levels in *BubR1*$^{H/H}$ MEFs. (A) Quantification of Cyclin B1 intensity in MEFs of indicated genotype following 1 hr treatment with DMSO, MG132, proTAME, or Apcin. (B) Same as (A). (C) Same as (A). Analyses in A-C were performed on three independent lines per genotype (10 cells per line). Data represents mean ± s.e.m. Statistical significance was determined in C using a two-tailed, unpaired *t*-test. **P* < 0.05 vs. WT DMSO. #*P* < 0.05 vs. BubR1$^{H/H}$ DMSO. ##*P* < 0.01 vs. BubR1$^{H/H}$ DMSO. *Nup88*^{T} indicates combined transgenic lines 11 and 13.

Figure S6_Naylor et al.

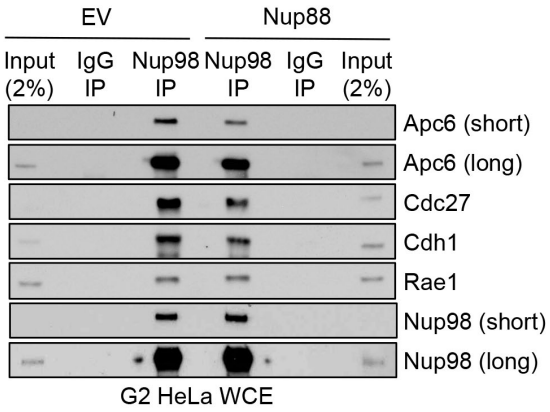

Figure S6. Figure 4. Nup88 sequesters Nup98-Rae1 away from APC/C^{Cdh1} during G2 phase when overexpressed. (A) Coprecipitation analysis of RO-3306-treated HeLa cells transduced with pTRIPZ-*HA-Nup88* (Nup88) or pTRIPZ-empty vector (EV) lentiviruses and immunoprecipitated with a Nup98 antibody. The Nup98 IP lanes are the same as shown in Figure 4C. Western blots are representative of three independent experiments. WCE, whole cell extract.

Figure S7_Naylor et al.

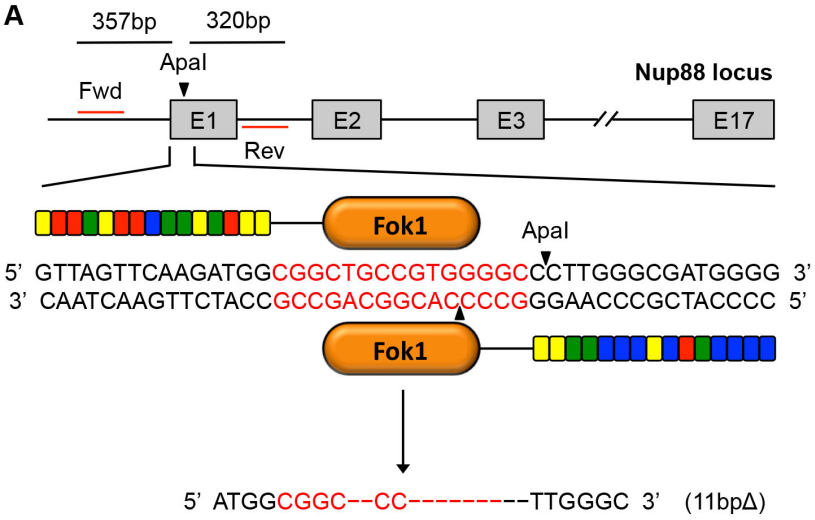

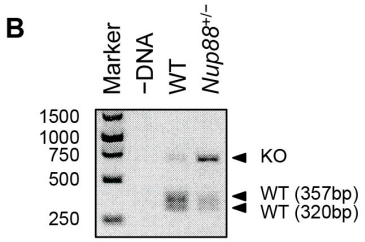

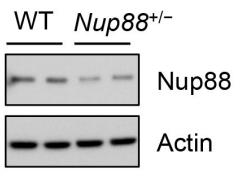

D

	***Nup88*$^{+/-}$ x *Nup88*$^{+/-}$ breeding**		
	Total progeny: 20		
	Nup88$^{+/+}$	*Nup88*$^{+/-}$	*Nup88*$^{-/-}$
Expected	5 (25%)	10 (50%)	5 (25%)
Actual	5 (25%)	15 (75%)	0 (0%)

Figure S7. Generation and characterization of *Nup88*$^{+/-}$ mice. (A) Schematic of *Nup88* TALENs, its DNA-binding sequences, and spacer (red). TALEN repeat variable di-residues (RVDs) are color-coded: NN (yellow), NG (red), NI (green), HD (blue). The resultant targeted mutation is shown with nucleotide deletions indicated by dashed lines. Four independent clones were isolated, three in-frame mutations and one frame shift mutation (shown). (B) Amplified genomic DNA was digested with ApaI and subjected to gel electrophoresis. Expected fragment sizes are indicated. (C) Western blot analysis of MEFs generated from *Nup88*$^{+/11bp\Delta}$ mice. (D) Expected versus actual genotypes of pups born from *Nup88*$^{+/11bp\Delta}$ x *Nup88*$^{+/11bp\Delta}$ breeding.

Figure S8_Naylor et al.

A

Mitotic MEF genotype (n)	Mitotic figures inspected	Aneuploid figures (%)	s.d.	Karyotypes with indicated chromosome number ≤39	40	≥41	Mitotic figures with PMSCS (%)	s.d.
WT (3)	150	9	1	7	136	7	1	1
Securin$^{-/-}$ (3)	150	15	1	10	127	13	6	1

B

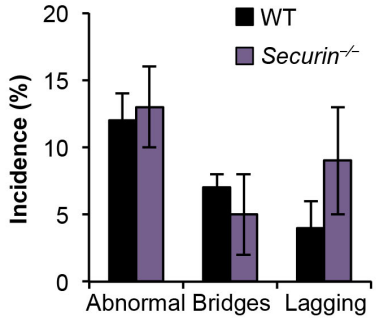

C

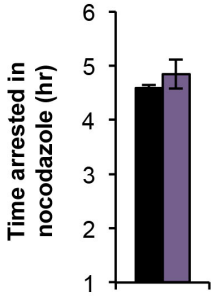

Figure S8. securin knockout MEFs have no mitotic abnormalities. (A) Karyotype analysis of numerical chromosomal abnormalities in passage 5 MEFs. (B) Analysis of chromosome segregation errors in MEFs expressing H2B-mRFP of the indicated genotypes. (C) Analysis of spindle assembly checkpoint activity of MEFs challenged with nocodazole. Analysis in A was performed on three independent lines per genotype (50 spreads per line). Analysis in B was performed on three independent lines per genotype (25 cells per line). Analysis in C was performed on at least three independent lines per genotype (>10 cells per line). Data represents mean ± s.e.m.

Figure S9_Naylor et al.

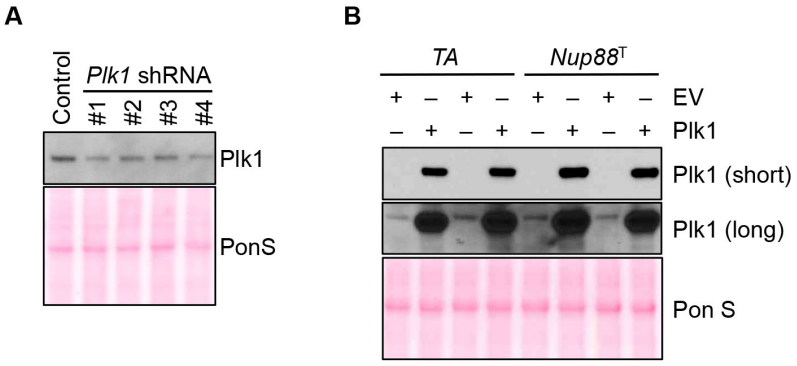

Figure S9. Lentiviral-mediated Plk1 knockdown and overexpression. (A) Western blot analysis of SV40 immortalized MEFs expressing one of four independent shRNAs against *Plk1* (see Figure 6A). (B) Western blot analysis of cells of indicated genotype overexpressing Plk1 (see Figure 6B).

Figure S10_Naylor et al.

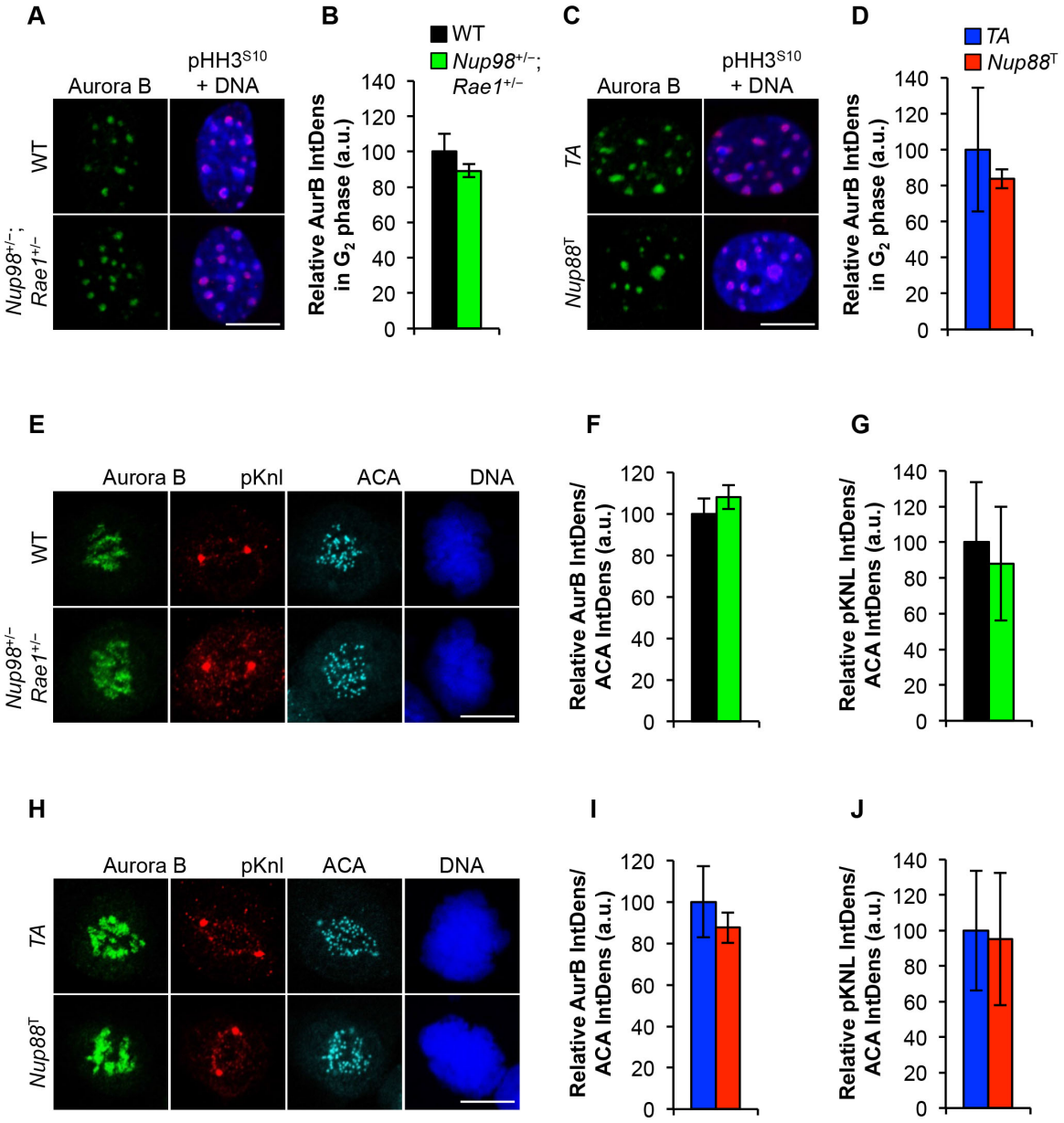

Figure S10. Aurora B protein levels and activity are unchanged in *Nup88* transgenic and *Nup98*$^{+/-}$*Rae1*$^{+/-}$ MEFs. (A) Representative images of G2 phase *Nup98*$^{+/-}$*Rae1*$^{+/-}$ MEFs immunostained for Aurora B. (B) Quantification of Aurora B intensity for cells in A. (C) Representative images of G2 phase *Nup88* transgenic MEFs immunostained for Aurora B. (D) Quantification of Aurora B intensity for cells in C. (E) Representative images of *Nup98*$^{+/-}$*Rae1*$^{+/-}$ MEFs in prometaphase immunostained for Aurora B, pKnl^{S24}, and centromeres. (F) Quantification of inner centromeric Aurora B intensity for cells in (E). (G) Quantification of outer kinetochore pKnl^{S24} intensity for cells in (E). (H) Representative images of *Nup88* transgenic MEFs in prometaphase immunostained for Aurora B, pKnl^{S24}, and centromeres. (I) Quantification of inner centromeric Aurora B intensity for cells in (H). (J) Quantification of outer kinetochore pKnl^{S24} intensity for cells in (G). DNA in A, C, E, and H was visualized with Hoechst. Analyses in B, D, F, G, I, and J were performed on three independent lines per genotype (25 cells per line). Data represents mean ± s.e.m. Scale bars = 10 µm. *Nup88*^{T} indicates combined transgenic lines 11 and 13.

Figure S11_Naylor et al.

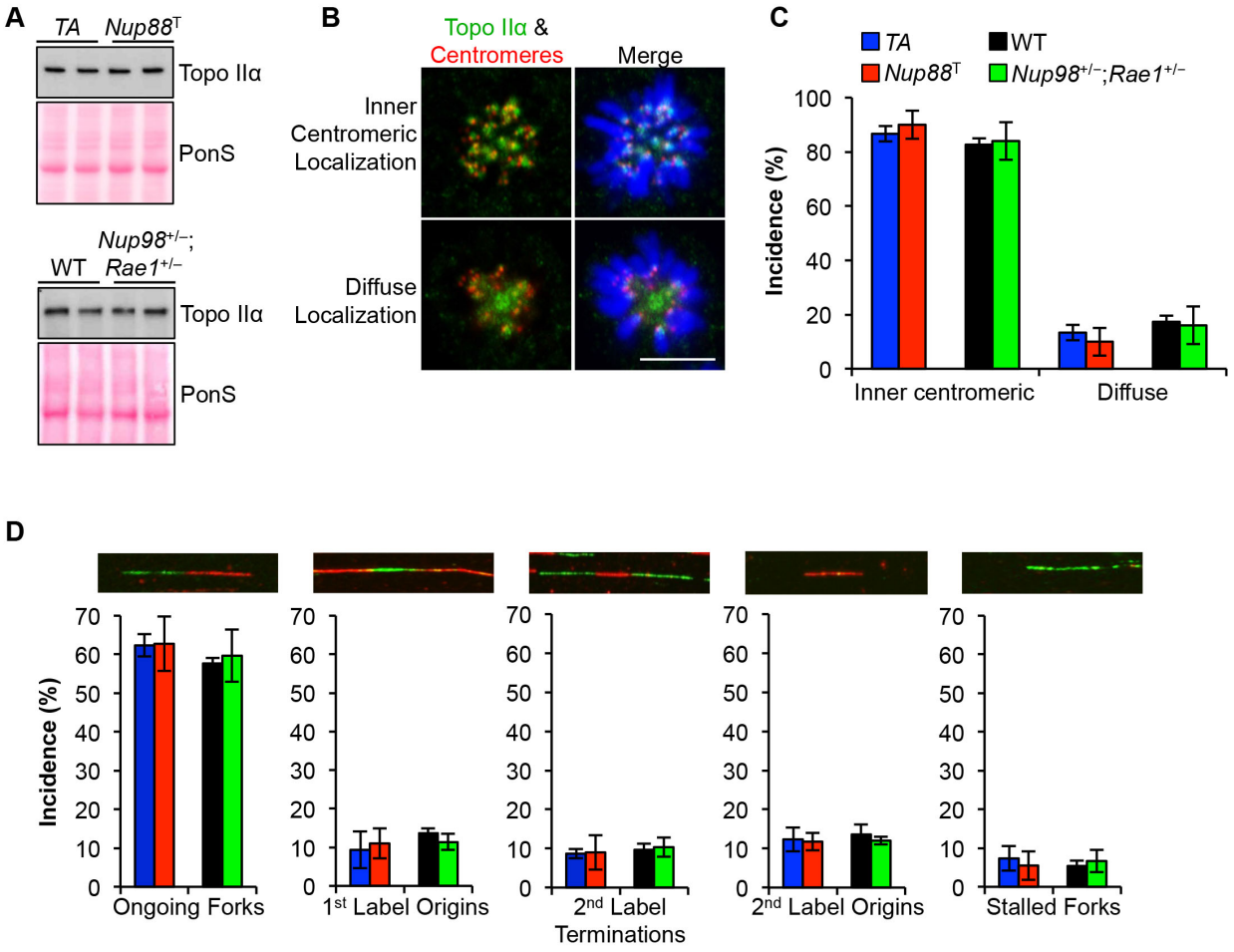

Figure S11. Topoisomerase IIα and DNA replication are normal in *Nup88* transgenic and *Nup98*$^{+/-}$*Rae1*$^{+/-}$ MEFs. (A) Western blot analysis of MEFs of the indicated genotype. (B) Representative images of *Nup88* transgenic MEFs immunostained for topo IIα and centromeres showing proper inner centromeric and diffuse localization of topo IIα. (C) Quantification of the incidence of inner centromeric versus diffuse topo IIα localization for *Nup88* transgenic and *Nup98*$^{+/-}$*Rae1*$^{+/-}$ MEFs compared to their respective controls. (D) Representative images of DNA fibers from *Nup88* transgenic MEFs and quantification of the incidence of each type of fiber classification for *Nup88* transgenic and *Nup98*$^{+/-}$*Rae1*$^{+/-}$ MEFs compared to their respective controls. DNA in B was visualized with Hoechst. Analysis in C was performed on three independent lines per genotype (25 cells per line). Analysis in D was performed on three independent lines per genotype (100 fibers per line). Data represents mean ± s.e.m. Scale bars = 10 μm. *Nup88*^{T} indicates combined transgenic lines 11 and 13.

Figure S12_ Naylor et al.

Lung fibroblast genotype (n)	Mitotic figures inspected	Percent aneuploid figures	SEM	Karyotypes with indicated chromosome number					
				38	39	40	41	42	80
TA (3)	75	8	2	0	3	69	1	0	2
Nup88 (3)	75	28	4	3	6	54	5	1	6

Figure S12. Nup88 overexpression causes aneuploidy in tumor-prone tissues. Karyotype analysis of numerical chromosomal abnormalities in cell cultures established from minced lung harvested from 5-month old transgenic mice (see Figure 9B).

Figure S13_ Naylor et al.

A. Normal Nup88 levels in late G2 phase

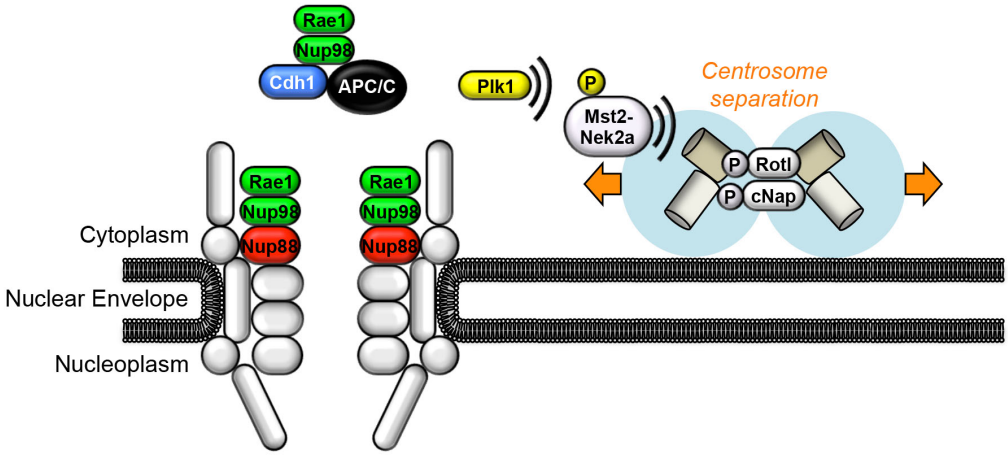

B. Elevated Nup88 levels in late G2 phase

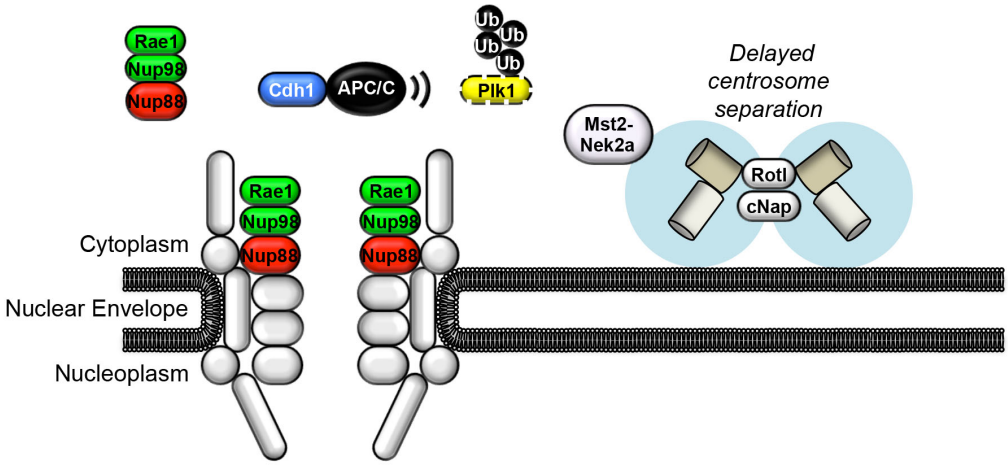

Figure S13. Proposed model for how the cytoplasmic Nup88-Nup98-Rae1 axis coordinates centrosome separation in late G2 phase by regulating pre-mitotic APC/CCdh1 activity. (A) When Nup88 protein levels are normal, soluble Nup98-Rae1 prevents APC/C^{Cdh1} from targeting Plk1 for proteolysis. Activated Plk1 phosphorylates Mst2-Nek2A to promote c-Nap1-mediated centrosome separation in late G2 phase. (B) When Nup88 protein levels are high, Nup88 accumulates in the cytoplasm and sequesters the inhibitory Nup98-Rae1 complex away from APC/C^{Cdh1}, thus promoting the proteasomal degradation of Plk1 prior to mitosis. Plk1 can therefore no longer promote c-Nap1-mediated centrosome separation through Mst2-Nek2A phosphorylation. This causes delayed centrosome separation, which induces chromosome missegregation through merotelic attachments and lagging chromosomes.